Mössbauer study of ball-milled Fe-Ge alloys

A. F. Cabrera and F. H. Sánchez
Departamento de Físíca, Instituto de Fisica de La Plata, Universidad Nacional de La Plata, C. C. 67, 1900 La Plata, Argentina
(Received 30 July 2001; published 1 February 2002)

In this work the mechanical alloying of $Fe_{100-x}Ge_x$ was studied as a function of alloying composition ($9 \leqslant x \leqslant 40$) processing time and annealing treatment. The alloys were prepared using a high-energy vibratory ball mill. For $9 \leqslant x \leqslant 27.5$ a single phase $A2$ solid solution was formed while for $x \geqslant 30$ besides the solid solution an increasing amount of disordered $B8_1$ (NiAs type) Fe_3Ge_2 was found. Thermally induced $A2 \rightarrow D0_3$ transition was investigated for $9 \leqslant x \leqslant 27.5$. The detailed annealing temperature dependence of short- and long-range ordering into the $D0_3$ structure was studied for the case of $Fe_{75}Ge_{25}$ by means of Mössbauer-effect spectroscopy and x-ray diffraction. The solid solution orders gradually and homogenously into the $D0_3$ structure. To follow and quantify the evolution of short-range order a special fitting routine for Mössbauer spectra was used that takes into account local and nonlocal contributions to the hyperfine interactions experienced by a ^{57}Fe probe, and that assumes nonlinearity dependences on the number of neighbors of a given class. By this means the short-range $D0_3$ order parameter S was determined for as milled steady states as well as annealed states for $9 \leqslant x \leqslant 27.5$. In the case of $Fe_{75}Ge_{25}$ the evolution of mechanical alloying with time was investigated. It was found that alloying proceeds in two stages. In the first one, iron rich (with $A2$ structure) and disordered Ge-rich regions coexist along with an almost equiatomic $A2$ Fe-Ge solid solution, which was interpreted as an interphase physically located between the former two. The three phases collapse into just one bcc solid solution with $S \approx 0.3$ for a critical time t_c, which was identified as the chemical mixing time reported by other authors. The second stage of mechanical alloying produces the complete homogenization of the solid solution. Plausible basic mechanisms of mechanical alloying of Fe-Ge mixtures are discussed on the basis of the results presented here.

DOI: 10.1103/PhysRevB.65.094202 PACS number(s): 75.50.Bb, 81.20.Ev, 81.30.Hd, 76.80.+y

I. INTRODUCTION

The synthesis and development of materials by mechanical alloying has been extensively studied during the last decade. The reasons for this intense activity, reflected in the nondecaying interest the subject maintains in frequently held scientific and technological meetings, are multiple. Mechanical alloying represents a nonexpensive versatile route able to produce equilibrium as well as nonequilibrium materials including amorphous, nanostructured, composites, and extended solid solution systems. In many cases high-energy mills are used, where starting materials are repeatedly submitted to severe deformation, fracturing, and welding. A feature common to a large number of systems is that these processes induce the refinement of the microstructure up to the nanoscopic scale while giving rise to interdiffusion and mixing of the reacting elements. The way mixing occurs was the subject of recent investigations in which the concepts of ''dislocation pumping solute''[1] and ''chemical mixing time''[2] have been coined and discussed. These concepts seem to be of great importance when homogeneity at a mesoscopic scale is achieved. At this critical stage the mixing reaction accelerates and completes within a relatively short period of time. In order to clarify and develop further these ideas it is necessary to obtain experimental information, as detailed as possible, on the way mixing proceeds.

Mechanothermal treatments of an alloy also introduce structural and chemical local and nonlocal changes. At an atomic location, the modification of the numbers of nearest and next-nearest neighbors of a given class is of prime importance, as these determine local properties such as atomic charge distribution and magnetic moment. Local properties are also affected by the system global changes such as variations of mean composition, average interatomic distances, etc., which have a direct influence on the electronic bands of the system. Therefore, Mössbauer-effect (ME) spectroscopy, being sensitive to the magnetic field (hyperfine field) and charge density (isomer shift) at the probe nuclei, becomes a powerful tool. It samples the material local and nonlocal changes induced by mechanical alloying and by thermally or mechanically activated ordering/disordering mechanisms. However, the problem is to find out an adequate spectral analysis procedure, which allows the retrieval of the relevant local and nonlocal information from complex patterns. The model applied in the past to iron-base-diluted magnetic alloys,[3,4] must be improved to take into account the hyperfine field and isomer shift nonlinear dependence with the number of atoms of a given class located at a given neighbor shell. Furthermore, some systems have the tendency to achieve a significant degree of order, even when they are produced by nonequilibrium routes that promote random atomic distribution, like mechanical alloying does.[5] For these systems, the analysis model must also consider the departure of atomic configuration probabilities from the ideal random ones.

In this work, we study mechanical alloying and ordering mechanisms of $Fe_{100-x}Ge_x$ systems ($9 \leqslant x \leqslant 40$). Work objectives are the investigation of (i) the composition dependence of the ball-milled and annealed steady states of the alloy, including estimations of maximum solid solubility of Ge in the bcc structure and degree of order departure from the random state; (ii) the way ordering from $A2$ to $D0_3$ structures proceeds; (iii) the evolution of the system with

mechanical alloying time in terms of the coexistence of terminal solubility phases and a hypothetical physical interphase created by mechanisms such as the proposed dislocation pumping solute one.

II. EXPERIMENTAL

$Fe_{100-x}Ge_x$ alloys, with nominal composition of $9 \leqslant x \leqslant 40$, were prepared by mechanical alloying (MA) from elemental constituents Fe (99.98–99.999% purity) and Ge (99.998% purity). Ball milling was performed at about 27 Hz with a Retsch MM2 horizontal vibratory mill using 10-cm^3 stainless steel vials with 12-mm balls of the same material. Samples of 700 mg were sealed into the milling vial under Ar (99.998%) atmosphere in a globe bag connected to a vacuum pump ($P \approx 4 \times 10^{-2}$ mbar) and to the Ar supply. The ball-to-powder mass ratio was about 10:1. For $x = 25$ at. %, in order to characterize the temporal evolution, different samples were prepared with milling times between 2–20 h. We confirmed that milling times of about 20 h were sufficient to achieve a steady state.

The study of composition dependence was performed in the range 9 to 40 at. % of Ge on samples mechanically alloyed during 10 h.

The alloys were characterized by means of Mössbauer-effect (ME) experiments and x-ray diffractometry (XRD). The Mössbauer spectra were recorded in transmission geometry using a constant acceleration spectrometer with a 10-mCi ^{57}Co Rh source. Two different methods were applied in order to describe the experimental spectra. In one case they were fitted using a large number of theoretical subspectra separated by regular magnetic-hyperfine-field (MHF) intervals [magnetic-hyperfine-field distributions (MHFD)]; a linear correlation between the values of MHF and isomer shift (δ) was assumed (MHFD program). In the other case, a program taking into account local and nonlocal spectral contributions, as well as the alloy state of order was employed (see the following section). All isomer shifts quoted are relative to α-Fe. X-ray-diffraction patterns were obtained with a Philips PW 1710 diffractometer using Cu $K\alpha$ radiation. All measurements were made at room temperature.

III. EVOLUTION WITH COMPOSITION AND ME ANALYSIS MODEL

We studied the stationary state for compositions $x = 9$, 14, 20, 22.5, 25, 27.5, 30, and 40. All samples were milled between 10–20 h.

For $x \leqslant 30$ the diffraction patterns (Fig. 1) show only four broad lines that can be associated to a bcc solid solution ($A2$) reflections. The (110) line becomes broader with the amount of germanium in the alloy for x up to 22.5. Its mean angular position decreases for x up to 20 but remains constant for higher Ge concentrations. The lattice parameter reflects the incorporation of Ge atoms into the bcc-Fe structure, it expands continuously from $a = 2.866$ Å (value for α-Fe) to $a \approx 2.902$ Å for $x = 22.5$ [Fig. 2(i)]. According to the equilibrium phase diagram[6] the $Fe_{1-x}Ge_x$ alloy system should have an α_1 phase region for $16 \leqslant x \leqslant 21$ and a two phase one ($\alpha_1 + \beta$) for $21 \leqslant x \leqslant 37$. However, the formation of only a disordered bcc phase in the as-milled alloys for $x = 25$ and 27.5 implies that the ball milling inhibits the formation of the hexagonal (β) phase and favors only the de-

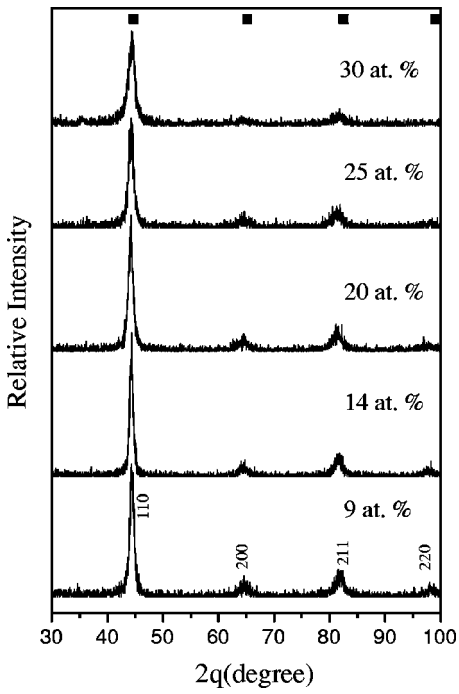

FIG. 1. X-ray-diffraction patterns of the MA stationary state (solid solution) of $Fe_{100-x}Ge_x$ ($9 \leqslant x \leqslant 30$). Squares indicate the position of the α-Fe bcc lines.

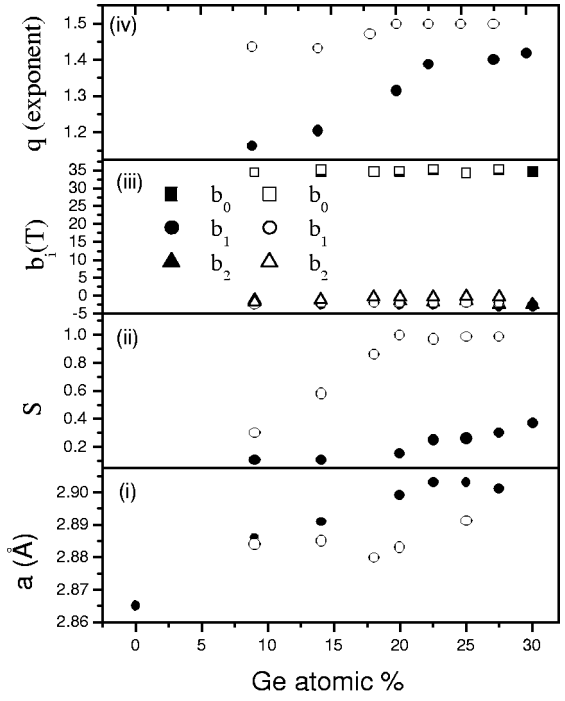

FIG. 2. Ge concentration dependence of lattice parameter a (i), short range order parameter S (ii), exponent q (iii) and hyperfine magnetic-field contributions b_i (iv). (● as-milled and ○ annealed samples).

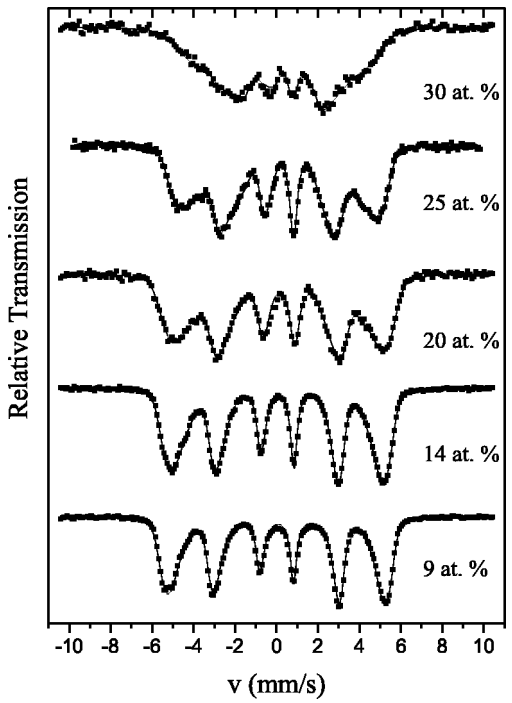

FIG. 3. Mössbauer spectra of the ball-milled $Fe_{100-x}Ge_x$ alloys. The solid lines represent the curves fitted with the $D0_3$ program.

velopment of the α-bcc structure. Mechanical alloying extends the compositional range of Ge random solubility from the typical 10% for alloys in thermodynamical equilibrium to 27.5% in the as-milled alloys of the present study. For $x=30$ besides the bcc reflections there is also a weak line located at about 36° (Fig. 1). This reflection is most probably due to the formation of a small amount of $B8_1$ (NiAs-type) Fe_3Ge_2 phase that appears more abundantly for $x=40$ (see below).

The Mössbauer spectra shown in Fig. 3 ($9 \leqslant x \leqslant 30$) become more intense at low Doppler velocity values and less

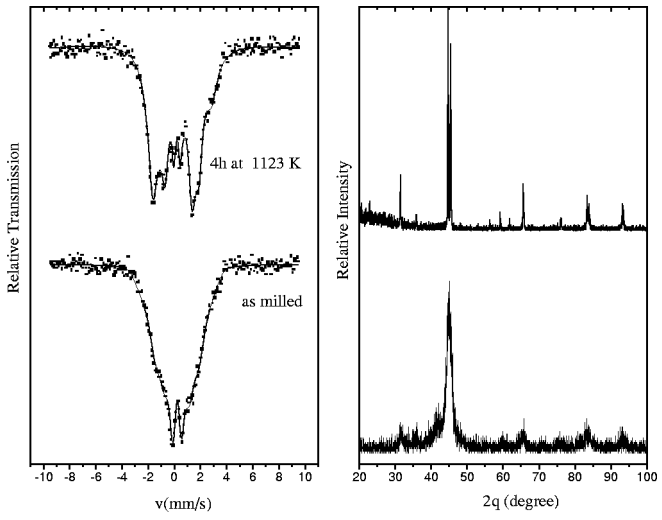

FIG. 4. Mössbauer spectra and x-ray diffraction corresponding to as-milled and thermally treated $Fe_{50}Ge_{40}$ samples. The solid lines correspond to the MHFD-program fits.

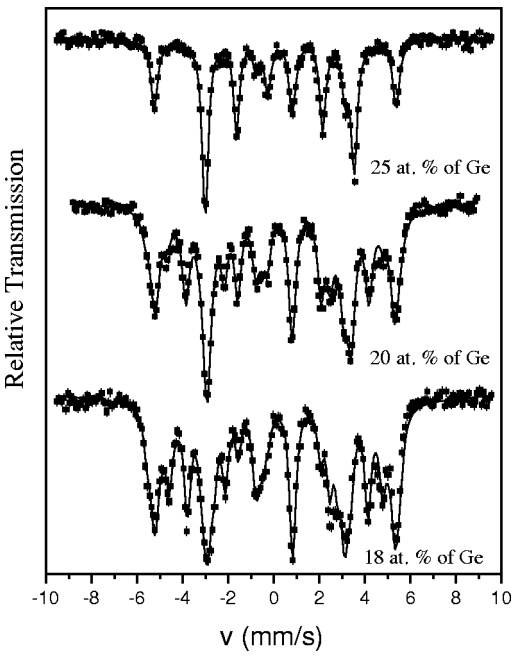

FIG. 5. Mössbauer spectra of $Fe_{100-x}Ge_x$ samples ordered at 673 K during 4 h; the solid lines correspond to the $D0_3$-program fits.

structured when the amount of germanium increases because the hyperfine-field distributions are continuously broadened and shifted towards smaller field values. This clearly indicates an increase of the probability of iron surroundings with randomly distributed germanium neighbors. All the spectra can be fitted with one magnetic hyperfine-field distribution, this distribution being associated with the almost random character of the bcc solid solution. The changes produced by the Ge concentration are more evident in the Mössbauer spectra than in the diffractograms, where the long-range order parameter is barely affected.

For $x=40$ the XRD and ME results indicate that the steady state is no longer a single phase but a mixture of the bcc solid solution plus a disordered hexagonal $B8_1$ (NiAs) Fe_3Ge_2 compound (Fig. 4). A thermal treatment of 4 h at 1123 K leads to the ordering of the system in the $B8_1$ structure; consistently with the global composition, no bcc solid solution is left.

Thermal treatments at 673 K during 4 h were performed to study the ordering of the samples. Partial $D0_3$ order was observed for $x=14$ while complete order was found for concentrations of 18, 20, 22.5, 25, and 27.5 at. % of Ge, beyond the Ge concentration range ($x \approx 16-21$) where the ordered phase is reported to be the equilibrium one.[6] The spectra of samples with $x=18$, 20, and 25 are shown in Fig. 5. From a careful examination of their relevant features and considering the reported change of the hyperfine field (B) with the number of Ge nearest (n) and next-nearest (m) neighbors,[7] as well as the expected probabilities $P(n,m,x)$ of the Fe sites local configurations, we estimated the contributions to B from several $(n,0)$ and $(0,m)$ configurations. The corresponding values are plotted in Fig. 6. B shows a nonlinear diminution with the number of Ge nearest neighbors, stronger than that occasioned by Ge next-nearest ones. A similar

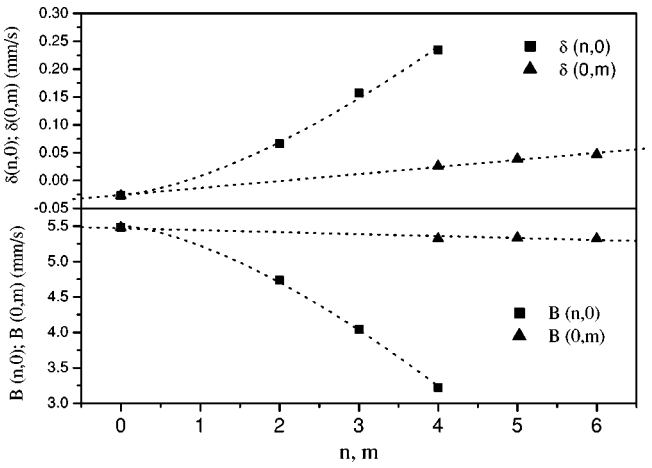

FIG. 6. Evolution of the B and δ with the number of the first and second Ge neighbors. The dotted lines are fits with function $y=y_0+y_1n^{1.5}+y_2m$, with y_i corresponding to b_i or δ_i.

behavior (but opposite in sign) is observed for the isomer shift $\delta(n,m)$ values. These results agree well with those previously reported for the Fe_3Si system.[8] The variations of B and δ with n and m, estimated from data shown in Fig. 6, were used in the present work as initial values for the analysis of ME spectra of samples with different composition and degree of order.

A linear correlation between hyperfine field (or isomer shift) and the local coordination numbers n and m:

$$B(n,m)=b_0+nb_1+mb_2,$$

$$\delta(n,m)=\delta_0+n\delta_1+m\delta_2,$$

has been used in the past for diluted iron-base solid solutions.[3,4] Some authors have used this correlation for describing $B(n,m)$ for compositions of up to 18 at.% of Ge. But in view of the nonlinearity of our results, we proposed a dependence n^q on the number of first neighbors, with q approaching unity for low Ge concentrations. From the fit of $B(n,0)$ and $\delta(n,0)$ (Fig. 6, $x=18-25$), the exponent q was proposed to be 3/2 for concentrations near 25 at.%. All the spectra were fitted with a specially developed routine using the following functions:

$$B(n,m)=b_0+n^qb_1+mb_2,$$

$$\delta(n,m)=\delta_0+n^q\delta_1+m\delta_2.$$

This fitting program ($D0_3$ program) takes into account two types of spectral contributions that different configurations around the Fe probes would produce. It has been probed that when the number of Ge first neighbors is larger than four there is no detectable magnetic Zeeman splitting of the nuclear levels. Then the contributions to the spectra for $n\geqslant 5$ are pure electric quadrupole interactions, while those corresponding to $n\leqslant 4$ are essentially magnetic ones. This leads to a maximum of 63 contributions, 35 of which are sextets and 28 doublets. The magnetic interactions were allowed to be perturbed with small quadrupolar interactions of average value ε. On the other hand, the pure quadrupolar interactions were evaluated for each configuration by assigning a nominal charge z_{Ge} and z_{Fe} to the Ge and Fe atoms, respectively. The probabilities $P(n,m,x)$ for the $D0_3$ order have been calculated in terms of the short-range order parameter S and the Ge concentration x. For that purpose, we considered the α, β, and γ $D0_3$ sublattices[9] and the associated P_α, P_β, and P_γ occupation probabilities for the Ge atoms (see Table I).

TABLE I. Occupation probabilities P_α, P_β, and P_γ for the Ge atoms in the sublattices α, β, and γ of the $D0_3$ structure.

	$x\leqslant 25$	$x\geqslant 25$
P_α	$(1-S)x/100$	$(1+3S)x/100-S$
P_β	$(1+3S)x/100$	$S+x(1-S)/100$
P_γ	$(1-S)x/100$	$(1-S)x/100$

The fitting function $F(n,m,v)$ was then built using standard magnetic sextet and electric quadrupole doublet functions $S(n,m,v)$ and $D(n,m,v)$ evaluated for the fields and isomer shifts corresponding to each configuration,

$$F(v)=\sum_{n=0}^{4}P(n,m,x)S(n,m,v)+\sum_{n=5}^{8}P(n,m,x)D(n,m,v).$$

In the fitting program the variables were b_i, δ_i $(i=0,1,2)$, q, S, x, the mean quadrupole shift ε, and the effective charge z_{Ge} (for iron $z_{Fe}=0$ was adopted and kept fixed). After an exploratory evaluation ε and z_{Ge} were kept fixed too for all compositions and states of order. Initial values for b_i and δ_i were taken from literature.[3,7] This makes a total of nine to eleven fitting parameters, a rather small number taking into account that up to 63 contributions are taking into account. The assumption of a physical model for the spectral distribution and the small number of variables employed make the fitting function less flexible than other ones based on histograms, where the many individual amplitudes are free to vary with just restrictions concerning the derivative of the envelope with MHF and the rate it goes to zero at the chosen MHF minimum and maximum values. This lack of flexibility will became apparent when discussing the intermediate stages of the $A2\rightarrow D0_3$ ordering of $Fe_{75}Ge_{25}$, but it is compensated by the physical information it allows to retrieve. As it will be seen later, the main spectral features are fairly described in all cases.

It was found that the order parameter S undergoes an important evolution with x in the case of thermally treated alloys [Fig. 2(ii)]. S increases continuously from $S=0.3$ to 1.0 for $9\leqslant x\leqslant 20$, and remains close to one for $20\leqslant x\leqslant 25$. For as prepared samples the S values evolve from 0.1 to 0.4, this fact may indicate that partial order is already obtained despite the mechanical work. This result may be due to a competition between thermally induced ordering and stochastic mechanical disordering, as reported previously.[5] It would explain why a higher degree of order is obtained for Ge concentrations above the threshold of the equilibrium α_1 region.

Fitted values for b_i show little difference between those corresponding to ordered and disordered samples and a slight

variation with Ge concentration [Fig. 2(iii)]. As can be seen the hyperfine-field contribution b_0 for Fe probes with no Ge in the first two neighbor shells is larger than that measured in pure Fe while b_1 and b_2 are negative with $|b_1|>|b_2|$; for example, $b_0=34.54\,\mathrm{T}$, $b_1\approx-2.36\,\mathrm{T}$, and $b_2\approx-1.67\,\mathrm{T}$ (ordered and disordered alloys), for $x=20$. The b_i quantities are in reasonable agreement (especially good in the case of b_1) with those reported in the literature.[7]

As for the isomer-shift behavior, δ_0 increases with x, from 0.0 to about 0.1 mm/s ($0\leqslant x\leqslant 14$) and then remains almost constant. δ_1 shows a well-defined evolution, decreasing from about 0.06 to 0.04 mm/s in the same composition range. δ_2 is harder to evaluate because a larger dispersion is obtained but its absolute value is smaller than δ_1 with a tendency to bear negative values.

The exponent q remains approximately equal to 1.48 for ordered samples, but increases continuously from about 1.15 (9 at. %) to 1.40 (22.5–30 at. %) for disordered alloys [Fig. 2(iv)].

IV. $D0_3$ SUPERSTRUCTURE

The results discussed indicate that thermal treatment at $T\approx 673\,\mathrm{K}$ during 4 h orders the as-milled $Fe_{75}Ge_{25}$ alloy ($A2$) into the metastable cF16-Li_3Bi ($D0_3$) type structure (see Fig. 5). The unit cell of this structure is composed of eight bcc pseudocells with a lattice parameter approximately twice of that of α-Fe. The Ge atoms occupy four of the eight subcells centers in a regular tetrahedral arrangement. In this structure there are two different ^{57}Fe sites, which are well distinguished by Mössbauer spectroscopy. One has population 1/3 (minority site), with zero Ge nearest neighbors (nn) and six next-nearest neighbors (nnn) and the other has population 2/3 (majority site), with four Ge nearest neighbors and zero next-nearest neighbors. These configurations have hyperfine parameters well differentiated, namely, $B=33\,\mathrm{T}$, $\delta=0.15\,\mathrm{mm/s}$ and $B=20\,\mathrm{T}$, $\delta=0.33\,\mathrm{mm/s}$ for the minority and majority sites, respectively.

We studied the $A2\rightarrow D0_3$ transformation induced by thermal treatments at temperatures between 373–673 K. During the ordering process, the probabilities of the local environments of the probe atoms change, giving rise to different combinations of configurations whose contributions produce rather complex Mössbauer spectra. Experimental spectra were analyzed with different fitting programs. The hyperfine-field distributions $P(B)$ obtained with the MHFD program are shown in Fig. 7. Distinct peaks in the Hyperfine magnetic-field distribution correspond to different numbers of first Ge neighbors around ^{57}Fe atoms. These peaks are not equally spaced, which is a further evidence of the nonadditive effect of the Ge nearest neighbors. The contribution corresponding to one Ge nn cannot be distinguished from that of zero Ge nn (Ref. 10) because the weaker effect of the Ge next-nearest neighbors broadens the corresponding signals and hinders their resolution. The two features between 20 and 33 T correspond to three and two Ge nearest neighbors. The main peaks (20 and 33 T) show a tendency to move towards higher B values with increasing order, due to the removal of configurations with Ge next-nearest neighbors (20 T) or with

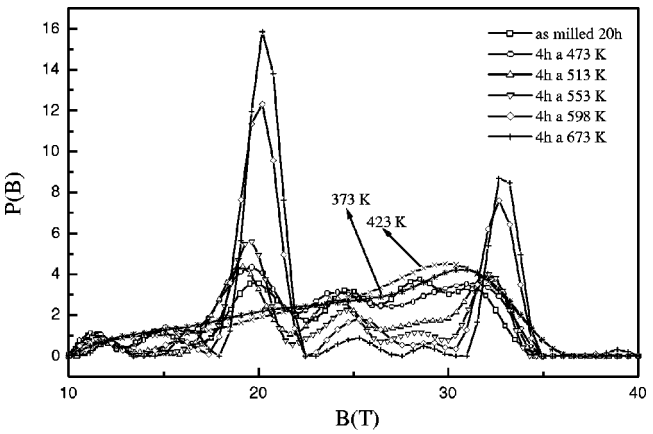

FIG. 7. ^{57}Fe hyperfine magnetic-field distributions $P(B)$ obtained with the MHFD program, as a function of thermal treatment temperature.

one Ge nearest neighbor (33 T). Moreover, the evolution of their relative intensities to a ratio close to 2:1 confirms the growth of the $D0_3$ order in the system. The fitted isomer-shift values are in accord with those reported by Hamdeh *et al.*[11] for partially ordered alloys.

We considered three different alternatives for the ordering into the $D0_3$ state: (a) $A2\rightarrow B2\rightarrow D0_3$ (existence of an intermediate ordered state); (b) $A2\rightarrow D0_3$ through coexistence of $A2$ and $D0_3$ regions; (c) $A2\rightarrow D0_3$ by gradual ordering. The best fits were obtained for the last assumption. The fitted spectra are shown in Fig. 8. In general, a fair description of the spectral evolution is obtained with this model; the largest

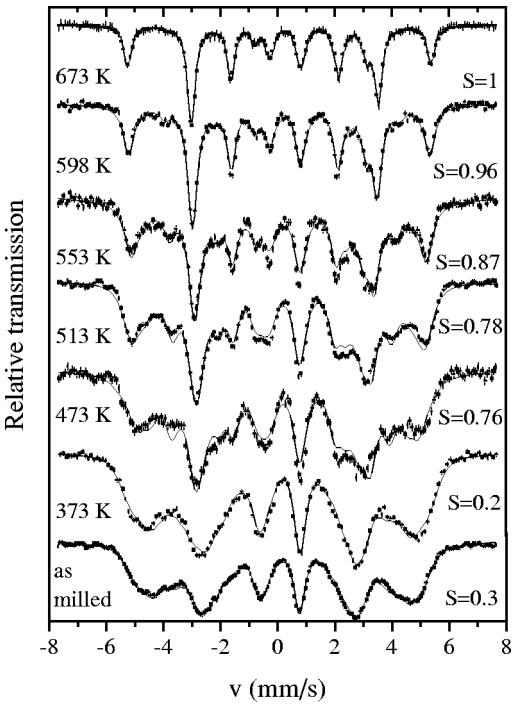

FIG. 8. Mössbauer spectra of the $Fe_{75}Ge_{25}$ alloys thermally treated at the indicated temperatures. The fits correspond to the $D0_3$ program. The fitted values of the short-range order parameter S are indicated.

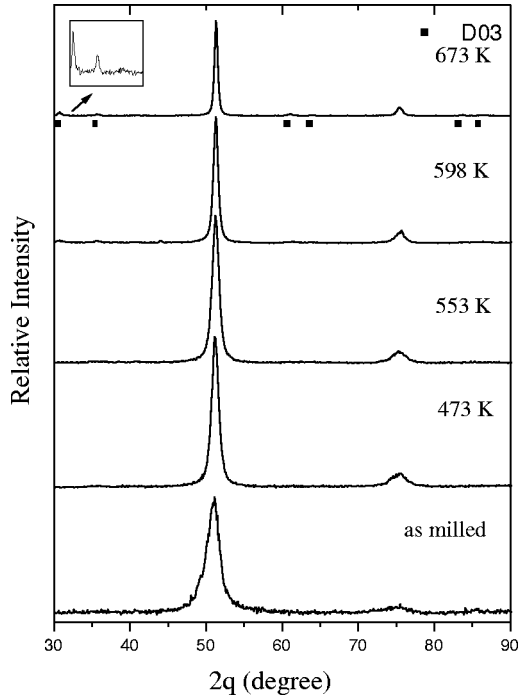

FIG. 9. XRD patterns of the $Fe_{75}Ge_{25}$ samples thermally treated at the indicated temperatures. The inset shows a detailed view of two of the $D0_3$ reflections.

deviations being observed for the sample treated at 473 K. This fact suggests that the gradual ordering assumption, even being the best of the three considered, is not entirely correct. The linewidths of the individual subspectra were allowed to become broader than the experimental resolution (typically 0.35 mm/s vs 0.24 mm/s for a 12-μm α-Fe standard absorber), in order to take into account contributions from mechanically induced defects. The fitting parameters b_0, b_1, and b_2 remain approximately constant with temperature, b_1 and b_2 having opposite sign to that of b_0:

$$b_0 = 34.6\ \mathrm{T},$$

$$b_1 = -2.17\ \mathrm{T},$$

$$b_2 = -0.75\ \mathrm{T}.$$

The parameters δ_i also remain nearly constant with mean values 0.105, 0.033, and 0.015 mm/s for $i=0$, 1, and 2, respectively. In almost all cases the dispersions are of the order of 1.2 T for b_i, 0.01 mm/s for δ_i ($i=1,2$) and 0.03 mm/s for δ_0.

The fit of the as-milled alloy spectrum suggests the existence of partial $D0_3$ order ($S=0.3$). S increases continuously with treatment temperature up to $S=1.0$ for $T=673\,\mathrm{K}$, with an important change between 373 and 473 K (see Fig. 8). The exponent q, stays approximately constant at 1.43, in agreement with what was mentioned for ordered and disordered samples in the range $9 \leqslant x \leqslant 30$.

The diffraction patterns (Fig. 9) show a decrease in the peak width as a function of temperature due to an increase of the average crystallite size and a decrease in the dislocation

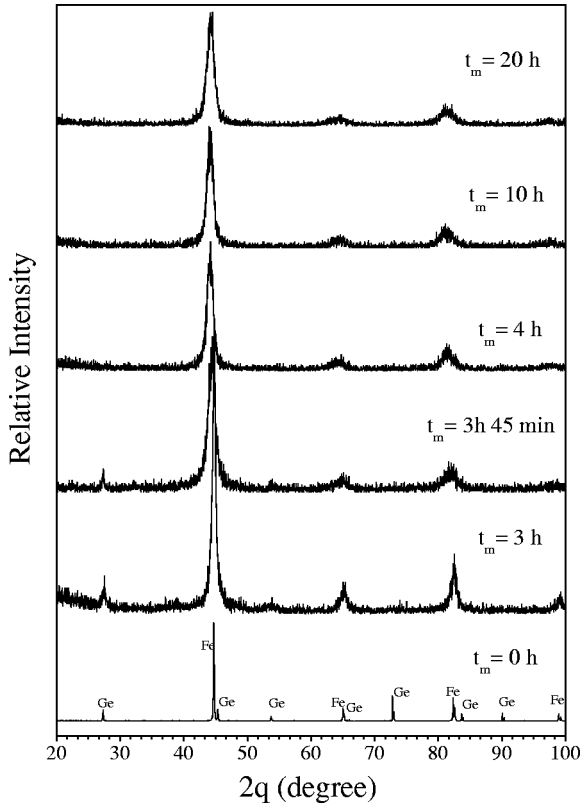

FIG. 10. X-ray-diffraction patterns of the $Fe_{75}Ge_{25}$ mixture mechanically alloyed during different times.

density and/or strain level. The diffractograms were measured with synchrotron radiation (LNLS, Campinas, Brasil) with $\lambda = 1.7652\,\text{Å}$, in order to allow the observation of the weak lines of the emerging $D0_3$ superstructure, by taking advantage of the high-intensity synchrotron radiation and the possibility of avoiding fluorescence from iron. The intensity ratio between the most intense superstructure/structure reflections agree with the theoretically estimated one $\mathrm{I}(111)/\mathrm{I}(220) \approx 0.003$.

Rietveld refinements of $D0_3$ base structure were performed, from which we obtained the evolution of the crystallite size, mean-square strain and lattice parameter with annealing temperature T_a. The thermal energy given to the system for $T_a \leqslant 598\,\mathrm{K}$ produces its ordering and recovery without promoting grain growth.[12] For $T_a = 673\,\mathrm{K}$ the mean-square strain continues decreasing while the crystallite size markedly increases. The $D0_3$ lattice parameter decreases continuously for temperatures up to 598 K and then remains constant at $a = 5.788\,\text{Å}$, but still larger than twice that of α-Fe, as expected for $D0_3$ Fe_3Ge.

V. TIME EVOLUTION OF MECHANICAL ALLOYING IN $Fe_{75}Ge_{25}$

We studied the alloy evolution with milling time (t_m) up to 20 h. Two steps can be clearly distinguished for $t_m < 4$ h and for $t_m \geqslant 4$ h, both by Mössbauer spectroscopy as well as by XRD.

The diffractograms are shown in Fig. 10. Diffraction lines

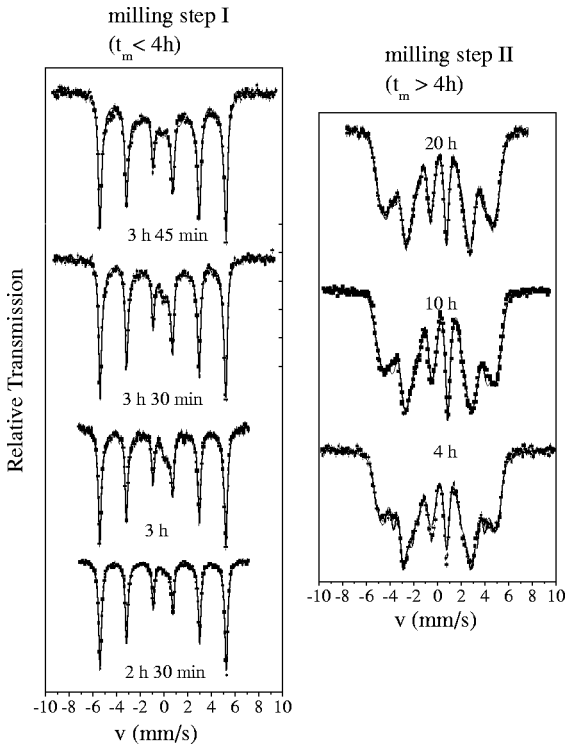

FIG. 11. Mössbauer spectra of the $Fe_{75}Ge_{25}$ powders obtained for different milling times. Full lines correspond to fits with the $D0_3$ program.

corresponding to bcc-Fe and fcc-Ge are observed for milling times smaller than 4 h. As the mechanical alloying time increases, the Bragg peaks of Ge disappear and only those corresponding to a bcc-Fe (Ge) solid solution are seen. The bcc peaks position is shifted to the left indicating the incorporation of Ge into the Fe lattice, moreover they became broader and shorter as a result of the refinement of crystallite size and the increase of internal strain. To separate these two effects, we used the method of integral breadth.[13] Initially, milling leads to a fast decrease of the grain size to about 210 nm (2 h 30 min) and to 7 nm (3 h) that then remains almost constant. The lattice parameter a was estimated by the Nelson-Riley method[14] using the diffraction lines (110), (200), and (211); it expands from 2.865 Å (α-Fe) to 2.9 Å [α-Fe (Ge)] showing a sudden change between 3 h 45 min and 4 h.[15]

The ME spectra for $t_m < 4$ h are well described with a sextet, of similar characteristics of that observed in α-iron and a doublet corresponding to a minor paramagnetic contribution (Fig. 11). The electric quadrupolar interaction with $\Delta = 0.52$ mm/s and $\delta = 0.36$ mm/s can be associated with a disordered Ge-rich phase. Disordered Ge-rich alloys have been reported to have similar parameters, for example, amorphous Fe_cGe_{100-c} ($18 \leqslant c \leqslant 27$).[16] In the first step of milling ($t_m < 4$ h) the hyperfine-field distribution broadens with milling time, appearing contributions with lower hyperfine fields while the relative intensity of the doublet increases. These facts suggest that the reaction progress occurs by means of two processes: the diffusion of Ge into Fe (diluted magnetic solid solution) and the diffusion of Fe into Ge (paramagnetic phase). The behavior observed for the mean values of hyperfine field and isomer shift of the magnetic component is in accord with that reported by Vincze and Aldred[4] for diluted alloys.

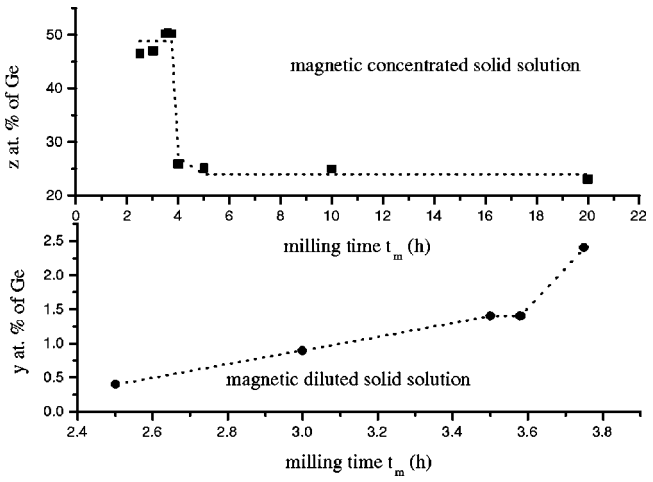

FIG. 12. Ge concentration dependence with milling time in the concentrated (z) and diluted (y) solid solutions that coexist in $Fe_{75}Ge_{25}$ samples for milling times $t_m < t_c \approx 4$ h.

Within the interval 4 h$\leqslant t_m \leqslant$20 h a randomlike supersaturated solid solution bcc-$Fe_{75}Ge_{25}$ forms and homogenizes. The spectra could be fitted with a hyperfine-field distribution[15] (with B from 10 to 40 T), whose associated isomer shifts agree well with those reported[17] for partially ordered solid solutions. For $t_m = 4$ and 10 h, fits with the $D0_3$ program show deviations from the experimental spectra (see Fig. 11). We interpret these deviations as an indication that the solid solution is not yet homogeneous, therefore, the model for a single bcc phase with partial $D0_3$ order is not entirely applicable for these milling times.

A closer look to the Mössbauer spectra ($t_m < 4$ h) suggests that besides the α-Fe-like interaction, the magnetic contribution includes a distributed minority component, with lower average hyperfine fields, which should correspond to environments richer in Ge. Its presence and growth can be inferred by noticing that ''valleys'' between the sextet lines depart progressively from the background level (see, for example, the spectra of the alloy after 3 h 45 min milling). A more detailed description of this situation can be achieved using a program similar to $D0_3$ program that admits the coexistence of the paramagnetic phase and two partially ordered solid solutions $Fe_{100-y}Ge_y$ and $Fe_{100-z}Ge_z$, and includes y and z as extra fitting parameters. In this approach the order parameter S is kept the same in both phases for the sake of simplicity (this restriction should not affect noticeably the description of the diluted magnetic component, as for the small Ge concentrations found there no significant changes are expected between ordered and disordered configurations).

The temporal evolution of Ge concentration in both magnetic phases is shown in Fig. 12, y changes from 0.5 to 2.5 from $t_m = 2$ h 30 min to $t_m = 3$ h 45 min for diluted solid solution while z (Ge concentrated solid solution) remains close to 50%. The exponent q was kept fixed at 1.0 and 1.5

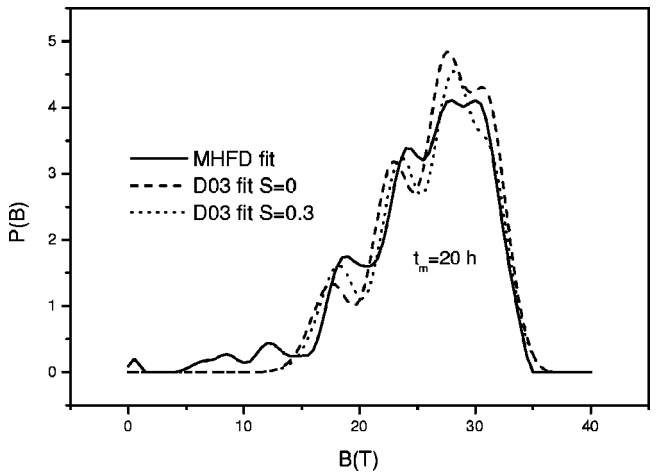

FIG. 13. Hyperfine-field distributions obtained with the two different fit programs.

for the diluted solution and for the concentrated one, respectively. The diluted solid solution contribution to the spectra diminishes with milling time and only one interaction with $x \approx 25$ was necessary to reproduce the signal for $t_m \geqslant 4$ h.

The mean hyperfine-field parameter values were $b_0 = 35.6$ T, $b_1 = -2.3$ T, and $b_2 = -1.5$ T for concentrated solid solution and $b_0 = 33.1$ T, $b_1 = -2.5$ T, and $b_2 = -1.2$ T for diluted solid solution. For the concentrated solid solution the isomer-shift contributions were $\delta_0 \approx 0.10$ mm/s, $\delta_1 \approx 0.04$ mm/s, and $\delta_2 \approx -0.01$ mm/s, while the nonlocal contribution for the diluted part was of the order of that of pure iron $\delta_0 \approx 0.01$, as expected.

Figure 13 shows the hyperfine-field distributions built using the fitted b_i values, along with the distribution obtained with a conventional histogram-fitting (MHFD) program. Good qualitative agreement was obtained between the two distributions, especially for an order parameter $S = 0.3$.

VI. DISCUSSION AND CONCLUSIONS

In the composition range $x \leqslant 30$ the samples obtained by 10–20 h MA show a mostly disordered bcc solid solution. The random solubility of Ge in Fe was increased by approximately 17% compared to what is predicted by the phase diagram.[6] The highest solubility obtained under our experimental conditions was 27.5 at. % of germanium. This fact is favored by the similarity of the atomic sizes of the two elements and the negative system mixing enthalpy (≈ -3 kJ/mole), but especially by the nonequilibrium preparation route. The Ge atoms incorporated in the iron structure produce an increase of the lattice parameter as well as changes in the mean hyperfine parameters: reduction of the hyperfine field and increase of the isomer shift. For samples with $x = 30$ and 40 besides the bcc solid solution a disordered hexagonal $B8_1$ Fe_3Ge_2 phase was encountered.

The contributions to the hyperfine field from first and second Ge neighbors in disordered, partially and totally $D0_3$ ordered samples show that its dependence with first neighbors is not linear and stronger than that of the second ones. The power-law exponent for the number of nearest neighbors n depends on concentration and degree of order, being higher (close to 1.5) for ordered samples and $x \geqslant 14$. The corresponding coefficient value, $b_1 \approx -2.36$ T, agrees fairly well with that estimated for diluted alloys, -2.34 T.[7] This agreement is not achieved when the exponent is forced to be equal to one. Although smaller, the MHF contribution b_2 per Ge second-nearest neighbor (as well as the δ_2 one, to the isomer shift), is important to give account of specific spectral features, such as the wide hyperfine interaction distribution observed in the as-milled samples. The b_0 values include a nonlocal contribution that is almost constant (though slightly growing with x) within the studied composition range. Its value is about 5% and 3% larger than $B(0,0)$ in pure iron and diluted Ge alloys,[4] respectively. Most probably this is partially due to magnetic coupling enhancement, originated in the lattice expansion resulting from the Ge addition. The effect of b_0 is observed in the high-field regions of the MHFD of disordered samples (see Fig. 7), and also in the B values of the large $(n=0, m=6)$ contributions developed in ordered samples with x next to 25. These values are close to that of pure iron $[B(0,6) \approx 33$ T] because of the competition between the opposite sign contributions from b_2 and b_0.

For $9 \leqslant x \leqslant 27.5$, the nonlocal contribution to isomer shift, increases within the ranges 0.06 mm/s$\leqslant \delta_0 \leqslant 0.14$ mm/s and 0.06 mm/s$\leqslant \delta_0 \leqslant 0.10$ mm/s, for as-milled and annealed samples, respectively. Again, a large part of the difference between these values and that of pure bcc-Fe can be ascribed to lattice expansion. Using the value reported by Ingalls[18] for the variation of δ with atomic volume Ω, $\partial\delta/\partial \ln \Omega \approx 1.33$ mm/s, we found

$$\Delta\delta_0^{\mathrm{vol}} = \delta_0^{\mathrm{vol}}(\text{as-milled}) - \delta_0^{\mathrm{vol}}(\text{annealed}) \approx (0.52 - 0.27\ \text{mm/s}) = 0.025\ \text{mm/s}$$

for samples with $x = 20$ to 25. This is about 60% of the difference of 0.04 mm/s obtained from the fits. The remnant 40% may be associated to band-structure ordering effects.

For $14 \leqslant x \leqslant 27.5$ the system orders into the $D0_3$ structure when submitted to a thermal treatment at a moderate temperature (673 K). The detailed study of the $Fe_{75}Ge_{25}$ system indicates that the $A2 \rightarrow D0_3$ ordering is mainly gradual and homogeneous, without passing through intermediate ordered states, such as $B2$. The change of the short-range order parameter S with annealing temperature is maximum between 373 and 473 K. The lattice constant constitutes a long-range order parameter, which also reflects the $A2 \rightarrow D0_3$ transition.

The temporal evolution of the mechanical alloying occurs in two steps, a properly alloying process, up to a critical time $t_c \approx 3.75$–4.00 h, followed by a homogenization process. For $t_m < t_c$ the mixture of Fe and Ge refines; the system microstructure scales down to a true nanostructure. Ball milling forces the continuously smaller grains of both elements to become in close contact. Then, within a narrow zone at both sides of the interface interdiffusion occurs. The mechanisms of interdiffusion are not well known, but most probably they are defect enhanced and nonthermally activated. Dislocation pumping solute[1] is a hypothetical process that may explain the situation. It will create solute supersaturated regions near interfaces as a consequence of rapid diffusion along disloca-

tions between ball impacts and rapid dislocation motion away from the solute-enriched zone during impacts. Within this frame, the supersaturated zone may be associated to the interphase with about 50% Ge found in the present work for $t_m < t_c$. It would separate the Fe-rich ($y < 2.5\%$ Ge) and Ge-rich regions. It is important to notice that the distinction between the interphase and the iron-rich solid solutions is extremely hard for x-ray diffraction, since both are bcc and highly chemically disordered. Therefore, the sensitivity of ME to short-range order along with the analysis method employed in the present work constitutes a great advantage for its detection and characterization. Ziller, Le Caër, and Delcroix[2] have proposed the concept of chemical mixing time also from ME results. In several bcc-based alloys prepared by MA they found out that the MHF distributions show common features for $t_m < t_c$. We have seen these features too, and conclude that a substantial contribution to them comes from the supersaturated interphase observed in the present work.

Time t_c is the one at which the fingerprints of the original components disappear. It was termed chemical mixing time by Ziller, Le Caër, and Delcroix.[2] At $t_m = t_c$ homogenization occurs due to energy minimization. This is achieved by the suppression of the large interfacial area when the steady-state solid solution is formed. At this time the lattice parameter shows a discontinuity attaining its final value. Results reported previously in Fe-M systems (M = Si, V, Cr, and Mn) (Refs. 12,19,20) can be interpreted within this frame. All these systems tend to produce steady states that consist of an $A2$ solid solution. The common features observed in their MHF distributions for $t_m < t_c$, may correspond to actual local configurations existing in the disordered interphase that separates the iron-rich bcc solid solution and the M-rich phase.

ACKNOWLEDGMENTS

The authors are grateful to CONICET, ANPCYT, and UNLP for partial financial support. We also wish to thank Dr. C. Cusatis from LNLS and Dr. M. Meyer from UNLP for the XRD high statistics measurements, as well as Dr. L. Mendoza Zélis from UNLP for kindly providing the quadrupole splitting nominal values corresponding to different (n,m) Ge configurations.

[1] R. B. Schwarz, Mater. Sci. Forum **269–272**, 665 (1998).
[2] T. Ziller, G. Le Caër, and P. Delcroix, Mater. Sci. Forum **312–314**, 33 (1999).
[3] L. Brössard, G. A. Fatseas, J. L. Dormann, and P. Lecocq, J. Appl. Phys. **42**, 1306 (1971).
[4] I. Vincze and T. Aldred, Phys. Rev. B **9**, 3845 (1974).
[5] P. Pochet, E. Tominez, L. Chaffron, and G. Martin, Phys. Rev. B **52**, 4006 (1995).
[6] E. Kato and S. Nunoe, in *Binary Alloy Phase Diagrams*, 2nd ed., edited by T. Massalski (ASM International, USA, 1996), Vol. 2.
[7] F. Van der Woude and G. A. Sawatzky, Phys. Rep., Phys. Lett. **12**, 5 (1974).
[8] M. B. Stearns, Phys. Rev. **129**, 1136 (1963).
[9] M. C. Cadeville and J. L. Morán López, Phys. Rep. **153**, 331 (1987).
[10] H. H. Hamdeh, S. A. Oliver, B. Fultz, and Z. Q. Gao, J. Appl. Phys. **74**, 5117 (1993).
[11] H. H. Hamdeh, M. R. Al-Hilali, N. S. Dixon, and L. S. Fritz, Phys. Rev. B **45**, 2201 (1992).
[12] A. F. Cabrera, Thesis, Universidad Nacional de La Plata, Argentina 1998.
[13] H. P. Klug and L. E. Alexander, *X-Ray Diffraction Procedures 661* (Wiley, New York, 1974).
[14] H. P. Klug and L. E. Alexander, *X-Ray Diffraction Procedures 594* (Wiley, New York, 1974).
[15] A. F. Cabrera, F. H. Sánchez, and L. Mendoza Zélis, Hyperfine Interact. **2**, 230 (1997).
[16] H. H. Hamdeh, M. R. Al-Hilali, N. S. Dixon, and L. S. Fritz, Phys. Rev. B **49**, 6312 (1994).
[17] B. Fultz, Z. Q. Gao, H. H. Hamdeh, and S. A. Oliver, Phys. Rev. B **49**, 6312 (1994).
[18] R. Ingalls, Phys. Rev. **155**, 2 (1967).
[19] T. Ziller, G. Le Caër, and P. Delcroix, J. Met Nan. Mat. **2–6**, 33 (1999).
[20] A. F. Cabrera, F. H. Sánchez, and L. Mendoza Zélis, J. Met Nan. Mat. **2–6**, 85 (1999).